Retinal Blood Vessels Segmentation for ROP Plus Form Diagnosis

José Almeida[1], Jan Kubicek[2], Martin Augustynek[2], Marek Penhaker[2], and Juraj Timkovic[3]

[1] FEUP - Faculty of Engineering of the University of Porto
Rua Dr. Roberto Frias, 4200-465 Porto, Portugal
[2] VSB–Technical University of Ostrava, FEECS, K450
17. listopadu 15, 708 33, Ostrava–Poruba, Czech Republic
[3] University Hospital Ostrava, Clinic of Ophthalmology
Ostrava, 708 52, the Czech Republic

Abstract. Eye diseases can have highly adverse outcomes without an early diagnosis and correct monitoring. Retinopathy of Prematurity (ROP) Plus Form, in particular, is a disease that can lead to childhood blindness, and its diagnosis requires medical experts to examine the retinal condition manually. Although developments in screening equipment have helped, this is still a time-consuming and subjective task. The development of automatic tools for Retinal Blood Vessel Segmentation allows the extraction of blood vessels from fundus images, which healthcare experts can then use to perform the diagnosis, monitoring, and prognosis of eye diseases. Thus, developing such a segmentation tool is a widely explored task with different methodologies that can be followed. However, many studies try to segment all the blood vessels rather than only the most important ones. In this work, we present a segmentation pipeline to segment only the main vessels whose characteristics can be used to assess ROP Plus Form disease. This pipeline uses different operations and filters, including CIELAB Enhancement, Background Normalization, Bell-Shaped Gaussian Matched Filtering, Modified Top-Hat operation, and Frangi Filtering. The final segmentation is done by determining a threshold value using the Triangle Threshold algorithm. The pipeline was tested in the well-known DRIVE Database, achieving an Accuracy of 0.949, Specificity of 0.963, and Sensitivity of 0.756.

Keywords: Retinopathy of Prematurity · Segmentation · Retinal Blood Vessels · Vessel Enhancement · Thresholding.

1 Introduction

Different eye diseases and conditions can be diagnosed and monitored by analyzing the condition of the patient's retina. Such diseases include Retinopathy of Prematurity (ROP), a well-known condition recognized as one of the leading causes of childhood blindness worldwide. While ROP can be subclassified into

different types, the Plus Form, characterized by high tortuosity, even in the main vessels, has been emphasized in recent studies. [5]

Traditional methods for assessing the state of such conditions were based on live diagnoses by ophthalmologists, which came with some issues like being time-consuming, not having the possibility to store retinal images for further evaluation, and having a higher risk of misdiagnosis.

Recent developments in screening methodologies have led to the design of fundus cameras. These allow for the acquisition of digital fundus images representing the subject's retina, which can then be sent and analyzed by ophthalmologists or even used for future studies in the area, making retinal imaging a cost-effective and more accurate approach for diagnosing and monitoring several diseases. [7]

Although a huge step has been made in this area with the adoption of such equipment, an expert's manual evaluation of the retinal images is still required, making the diagnosis and monitoring time-consuming and even subjective to a certain degree.

This makes Automatic Retinal Blood Vessel Segmentation an essential field of study, as it helps separate blood vessels from the remaining image. Using the segmentation result, a medical expert can analyze blood vessels' size, shape, and structure. Such characteristics are essential for diagnosing and monitoring different eye diseases and performing a prognosis, as changes in blood vessels can help doctors predict the development of a disease and provide patients with early treatment.

2 Related Work

By analyzing the literature, it became clear that segmentation methods can be divided into several groups. [8]

Region-based deformable models use a given region's internal and external forces and other statistical parameters to identify the objects and the background. Methods such as Chan Vase, Local Binary Fitting, and Active Contours [1] are included in this group.

Kernel-based methods are typically used to pre-process images and rely on developing filters and applying them through convolution. The output of such filters provides information about the structure and limits of the vessels. As these filters are explicitly designed to detect specific patterns, the term Matched Filter is usually employed. Some available filters are Gaussians [3, 15] and Difference of Gaussians [11]. Multi-scale segmentation is another group of segmentation methods also based on filters. However, they are intended to identify geometric patterns at different scales, allowing objects of different sizes to be recognized. This can be performed, for example, by applying multiple Gaussian-based filters with varying values of sigma. [6, 10, 12]

The fourth group is the Morphologic-based segmentation. In this case, methods use mathematical operations to enhance specific image structures. These

operations include erosion, dilation, skeletonization, opening, closure, and others derived from the combination of these [11]. Morphological processes depend on structural elements, which makes the segmentation based on the geometrical characteristics of the objects.

Adaptive thresholding allows image segmenting using different threshold values in different image regions. This is helpful for images with low brightness homogeneity. However, these methods are susceptible to noise and artifacts, making combining them with image preprocessing steps essential. Adaptive Otsu thresholding uses the intensity information of gray images to compute the threshold values in each section. The Joint and Local Relative (JRE and LRE) Entropy thresholdings [4, 15] use the GLCM of the image. Some methods also use the information from the output of wavelet transforms and Gaussian filters.

The methods mentioned above are part of the so-called Unsupervised Methods. The different methods can be combined to create different segmentation pipelines. The main advantage of such pipelines is that they do not require gold standards or annotated data to be developed. However, they need some pre-knowledge that helps establish the best image features for the task.

In recent years, one last segmentation group has received increased focus: Supervised Deep Learning. Many authors also explore using such models for retinal blood vessel segmentation, which includes, for example, using CNNs and CVANNs. [2, 9] Supervised learning methods usually achieve higher accuracy than unsupervised methods. However, more data and manual annotations are needed to train robust models, which can be an issue in many cases, especially in Biomedical Engineering. Thus, using Unsupervised Methods has the advantage of not needing training data.

It was also noticeable the use of the DRIVE Database [14] as a gold standard and the use of Accuracy, Specificity, and Sensitivity as preferred metrics to assess the segmentation performance.

3 Materials and Methods

In this work, we propose a novel Retinal Blood Vessel Segmentation Pipeline that extracts the essential vessel information from retinal images, which can be used to assess eye diseases such as the ROP Plus Form.

3.1 DRIVE Database

The DRIVE Database [14] is the most widely used for developing and testing Retinal Blood Vessel Segmentation algorithms.

This database contains two sets of fundus images, a training and a test set, with 20 images each. Both training and test sets include FOV masks for each image. However, only the training set contains manually annotated blood vessel masks that can be used as Ground Truth (GT) to compute performance metrics.

Fig. 1 shows an image example from the DRIVE Database.

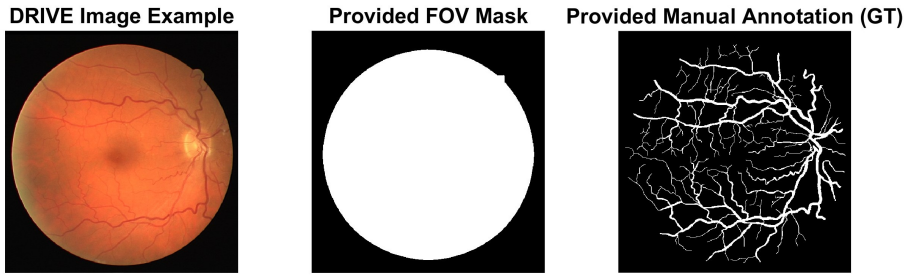

Fig. 1. Image 22 of the training set from DRIVE Database, its FOV Mask and Manual Annotation

3.2 FOV Mask generation

The visual information in retinal images is restrained to the Field of View (FOV), making it essential to have an FOV binary mask that can focus all other segmentation steps in this area. By accounting for the fact that, in every image, the outside of the FOV is always black, the mask can be generated by applying the Otsu Thresholding on the green channel of the raw RGB image. To the resulting binary image, firstly, a fill operation is used to ensure we have a complete disk within the FOV without any holes. Secondly, an erosion with a disk with radii ten as a structure element is also applied. Both these steps are essential since gradient-based operations will be used in the part of the image identified as FOV by the generated mask. If black holes existed or the border between the FOV and the outside were contained, it could lead to errors in the segmentation.

3.3 Image Preprocessing

Like many other approaches found in the literature, the first part of the pipeline should be the preprocess of the retinal images, which should allow the standardization of the image's brightness and contrast and better separate the objects from the background. The preprocessing of the images can be divided into several steps.

CIELAB Enhancement The first preprocessing step of the proposed pipeline is to perform a color enhancement based on the CIELAB color space. Specifically, the RGB image is converted to the CIELAB color space, and then CLAHE is applied to the L* Channel, which translates the perceptual lighting of the image. The image is then converted back to RGB. This allows for better discrimination between vessels and the background, as shown in Fig. 2.

Green Channel Extraction Like many other studies found in the literature, we opt to use the Green Channel of the enhanced image in the remaining steps

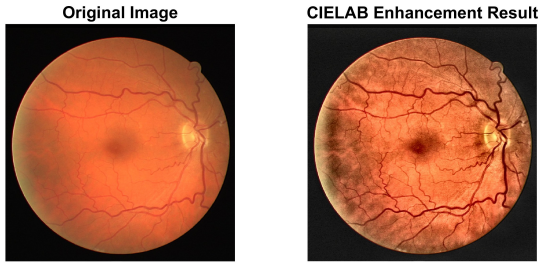

Fig. 2. Result of CIELAB L* Channel Enhancement applied to a Retinal Image

of the pipeline. This is mainly due to the increased discrimination between blood vessels and other background objects when using this channel rather than the red or blue channels.

Background Normalization A Background Normalization is then applied to the gray image to eliminate the main differences in intensities and overall background noise. The normalized image is obtained by the difference between the gray image and its background estimation, which can be computed by applying a sufficiently large mean kernel to the image. An example of this operation is represented in Fig. 3. [11]

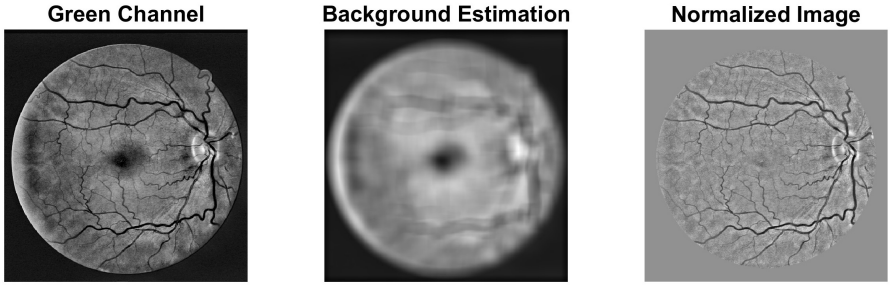

Fig. 3. Image's green channel (left), background estimation (middle), and the result of Background Normalization (right)

3.4 Vessel Enhancement

After preprocessing the image, different successive steps are applied for vessel enhancement. This part of the pipeline should allow us to get an image that is

easier to discriminate between the objects we want to segment and the rest of the information inside the FOV.

Bell-Shaped Gaussian Matched Filter The BSGMF has been used before for Retinal Blood Vessel Segmentation [15]. Its effect is enhancing the image's objects, especially the vessel-like structures, and removing other background information.

BSGMF is based on the kernel given by Eq. 1.

$$K(x, y) = \pm exp(-\frac{x^2 + y^2}{2\sigma^2}) \tag{1}$$

Its effect on a gray retinal image is represented in Fig. 4.

Modified Top-Hat A Modified Top-Hat Operation has also been proposed for Retinal Blood Vessel Segmentation [11], given by Eq. 2.

$$TopHat = I - min((I \bullet S_c \circ S_o; I) \tag{2}$$

Where $\bullet$ and $\circ$ represent the closing and opening operation, respectively, and S_c and S_o are the correspondent Structural Elements (SE). I is the input gray image.

Using this modified version of the well-known Top-Hat operation allows the enhancement of objects with a specific width, controlled by the size of the opening SE, while reducing the risk of enhancing other background elements. In our case, this operation was applied three times with increasing opening SE (from a disk with radii one through three) and with the closing SE as a disk with radii one. The three resulting images are then combined into one by averaging. The result of this operation is also represented in Fig. 4.

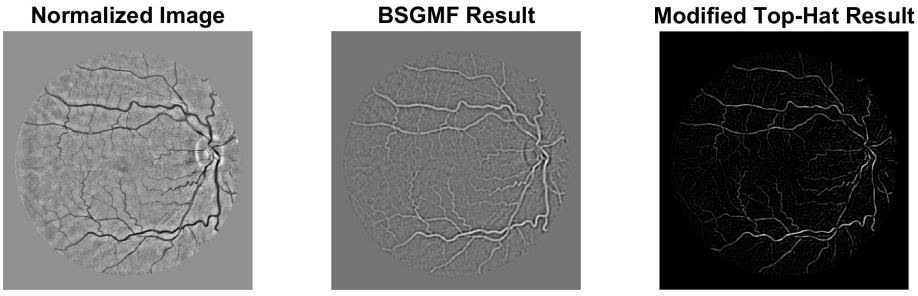

Fig. 4. Normalized image (left), BSGMF result (middle), and the result of applying the Modified Top-Hat operation to it (right)

Frangi Filter This Hessian-based Filter, proposed by Frangi et al. [6], was specially designed to enhance vessel-like structures. It can be mathematically described by:

$$V_{Frangi} = \begin{cases} 0, & \text{if } \lambda_2 > 0. \\ exp(-\frac{(\lambda_1/\lambda_2)^2}{2\beta 1^2})(1 - exp(-\frac{\lambda_1^2+\lambda_2^2}{2\beta 2^2})), & \text{otherwise.} \end{cases} \quad (3)$$

Where λ_1 and λ_2 are the eigenvalues of the image's Hessian Matrix. The computation of this matrix depends on a Gaussian Function used, which in turn depends on its standard deviation (σ). Therefore, σ is a variable that needs to be set for applying this filter. $\beta 1$ and $\beta 2$ are the other two parameters that must be manually set.

The eigenvalues, λ_1 and λ_2, are directly correlated to the vessel properties as they can be used to identify the presence of blood vessels: a λ_1 near zero and a negative λ_2 indicate the existence of bright tubular elements, in this case the blood vessels.

Applying this filter to the result of the modified Top-Hat operation allows almost perfectly to eliminate any object and information that is not a vessel. It also has an essential role in filtering between main vessels and branches, making it possible to control the relative response between both by changing its parameters.

Fig. 5 shows the result of applying the Frangi Filter to the image obtained in the last step. With close attention, it is possible to see that the image on the right still contains some background noise, whereas the image on the left, the result of applying the Frangi Filter, is almost clear of this noise and only includes the body of the blood vessels.

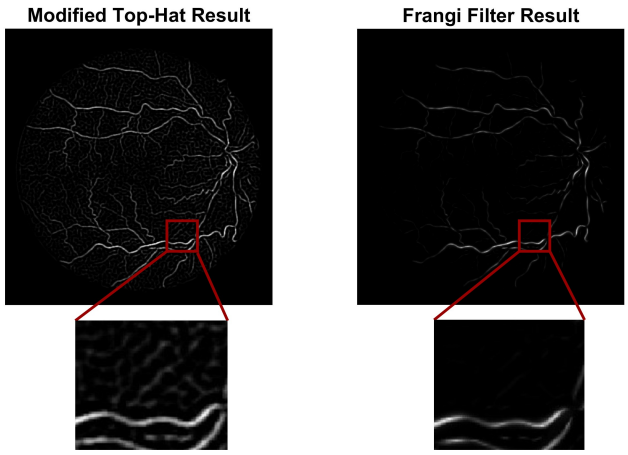

Fig. 5. Result from applying the Modified Top-Hat operation (left) and the result of applying the Frangi Filter to it (right)

3.5 Triangle Thresholding

A robust pipeline for vessel enhancement should allow for better discrimination between the blood vessels and other objects or background noise.

Thus, a thresholding method can perform well in segmenting the retinal blood vessels. The method chosen for our pipeline is the Triangle Thresholding. This method allows to compute a threshold value for images and signals based on a histogram with N bins, where N should be tested and set for each case. The threshold value is computed as follows: a line is drawn between the first non-zero and maximum histogram values. Then, the point of the histogram that distances the most to that line is determined. The abscissa of that point, which translates into a brightness value, is our threshold value. [13]

This method is ideal for images where the background has a well-defined, concentrated range of intensities and is separated from the objects' intensities in the image histogram. Thus, this method should perform well in the segmentation of images, such as the result of applying the Frangi Filter.

Lastly, the binarization result was also filtered to remove the smaller objects.

The complete proposed pipeline is represented in Fig. 6.

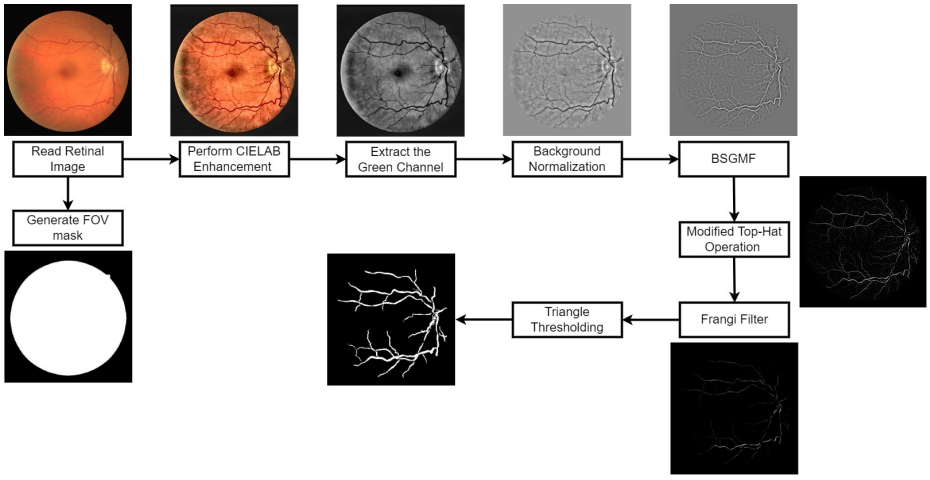

Fig. 6. Proposed Retinal Blood Vessel Segmentation in RetCam3 Images

3.6 Performance Assessment

Different segmentation metrics were used to assess the proposed methodology's performance.

The three most used metrics for performance assessment of segmentation pipelines are Accuracy (*acc*), Sensitivity (*sen*), and Specificity (*spe*). These metrics can be calculated as follows:

$$acc = \frac{TP + TN}{TP + TN + FP + FN} \tag{4}$$

$$sen = \frac{TP}{TP + FN} \tag{5}$$

$$spe = \frac{TN}{FP + TN} \tag{6}$$

Where TP and TN are the true positive and negative pixels, and FP and FN are the false positive and negative pixels, correspondingly.

4 Results and Discussion

The pipeline was tested to find the best parameter configuration for the DRIVE Database images.

The results presented in this section were obtained with a kernel size of 30x30 pixels for the Background Normalization, a 15x15 kernel with σ set as 2 for the BSGMF, and SE as a square with side 2 for the closing in the modified Top-Hat. The Frangi Filter was performed four times for each image with the σ values ranging from one to seven, with $\beta 1 = 0.5$ and $\beta 2 = 15$. Finally, the Triangle Threshold was applied with 128 bins.

Different segmentation results, the original images, and the provided GTs are represented in Fig. 7.

By visual analysis of the results, the pipeline achieved what was expected: the segmentation of the main vessels, with slight inclusion of smaller vessels and background noise.

The mean and standard deviation of the metric scores for the 20 images of the training set from the DRIVE Database can be found in Table 1, as well as the results of other works based on unsupervised methods that are available in the literature.

Accuracy and Specificity both achieve high mean scores and low standard deviation, which may confirm the effectiveness and robustness of the proposed pipeline. However, Sensitivity did not achieve a high mean score or a low standard deviation. By looking into how this metric is computed (Eq. 5), it is possible to see that it highly depends on the relation between TP and FN pixels. Since we tried to remove secondary vessels from the final segmentation, the amount of FN should be naturally higher, lowering the Sensitivity score. Moreover, the amount of secondary vessels may vary from image to image, which explains the high standard deviation obtained for this metric. The other two metrics are unaffected since the accuracy dependence on FN is low, as it considers the whole set of pixels in the image. Specificity only depends on TN and FP, which are not affected by the non-segmentation of secondary vessels.

Nevertheless, the obtained Accuracy and Sensitivity scores for the proposed pipeline outperform all the methods it was compared to. Specificity is also higher than most of the works, with only the pipeline proposed by Mendonça

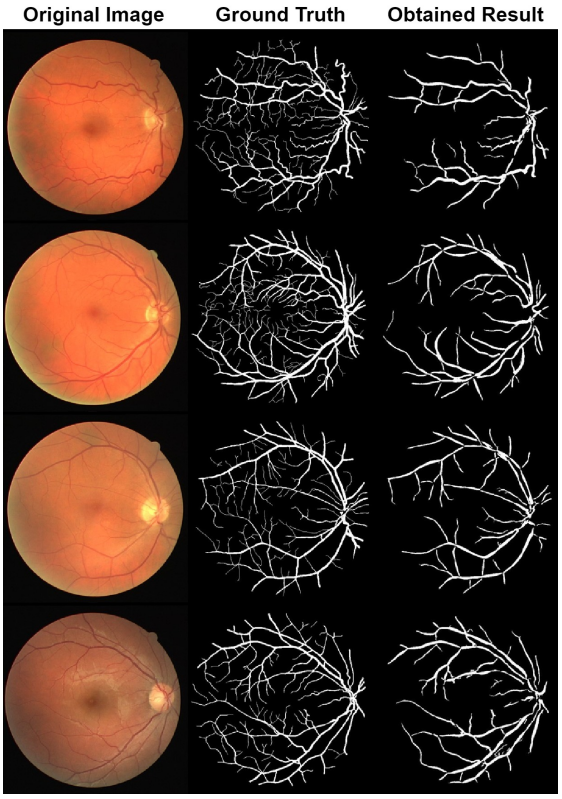

Fig. 7. Original DRIVE Image example(left), segmentation result with the proposed pipeline (middle), and Ground Truth (right)

Table 1. Comparison of Segmentation Scores based on the DRIVE dataset

Authors	**Metric**		
	Acc	Spe	Sen
Proposed Method	0.949 ± 0.009	0.963 ± 0.011	0.756 ± 0.055
Palomera-Perez et al. [12]	0.922	0.961	0.660
Al-Diri et al. [1]	0.926	0.955	0.728
Matinez-Perez et al. [10]	0.934	0.965	0.724
Chakraborti et al. [3]	0.937	0.958	0.721
Chanwimaluang and Fan [4]	0.932	0.959	0.660
Mendonça et al. [11]	0.945	0.976	0.734

et al. achieving a slightly higher result than ours. This comparison confirms our pipeline's effectiveness in segmenting the blood vessels from fundus images.

5 Conclusion

In this work, we proposed a Pipeline for Automatic Retinal Blood Vessel Segmentation to segment the main vessels of retinal images. The results confirm that this goal was achieved and that the pipeline shows high robustness and good performance.

Further testing should be made to see how this methodology generalizes for different image sources, especially retinal images from newborns, which are known to contain more noise and be less concise regarding brightness, contrast, and other core characteristics.

Particularly with the growing popularity of Deep Learning, the segmented images could be used to build tools for the automatic diagnosis and monitoring of diseases, such as ROP Plus Form. This should significantly impact healthcare, as it could make it less time-consuming and more independent of a medical expert's subjectivity.

Acknowledgement. The work and the contributions were supported by the project [SV4502261/SP2022/98] 'Biomedical Engineering systems XVIII'. This article has been produced with the financial support of the European Union under the LERCO CZ.10.03.01/00/22_003/0000003 project via the Operational Programme Just Transition.

References

1. Al-Diri, B., Hunter, A., Steel, D.: An active contour model for segmenting and measuring retinal vessels. IEEE Transactions on Medical Imaging **28**, 1488–1497 (2009). https://doi.org/10.1109/TMI.2009.2017941
2. Ceylan, M., Yacar, H.: Blood vessel extraction from retinal images using complex wavelet transform and complex-valued artificial neural network. 2013 36th International Conference on Telecommunications and Signal Processing, TSP 2013 pp. 822–825 (2013). https://doi.org/10.1109/TSP.2013.6614053
3. Chakraborti, T., Jha, D.K., Chowdhury, A.S., Jiang, X.: A self-adaptive matched filter for retinal blood vessel detection. Machine Vision and Applications **26**, 55–68 (1 2015). https://doi.org/10.1007/S00138-014-0636-Z/TABLES/6
4. Chanwimaluang, T., Fan, G.: An efficient blood vessel detection algorithm for retinal images using local entropy thresholding. Proceedings - IEEE International Symposium on Circuits and Systems **5** (2003). https://doi.org/10.1109/ISCAS.2003.1206162
5. Fleck, B.W., McIntosh, N.: Retinopathy of prematurity: Recent developments. NeoReviews **10** (2009). https://doi.org/10.1542/neo.10-1-e20
6. Frangi, A.F., Niessen, W.J., Vincken, K.L., Viergever, M.A.: Multiscale vessel enhancement filtering. Lecture Notes in Computer Science (including subseries Lecture Notes in Artificial Intelligence and Lecture Notes in Bioinformatics) **1496**, 130–137 (1998). https://doi.org/10.1007/BFB0056195/COVER

7. Karkhaneh, R., Ahmadraji, A., Esfahani, M.R., Roohipour, R., Dastjani, A.F., Imani, M., Khodabande, A., Ebrahimiadib, N., Ahmadabadi, M.: The accuracy of digital imaging in diagnosis of retinopathy of prematurity in iran: A pilot study. Journal of Ophthalmic and Vision Research **14**, 38–41 (1 2019). https://doi.org/10.4103/jovr.jovr_187_17
8. Krestanova, A., Kubicek, J., Penhaker, M.: Recent techniques and trends for retinal blood vessel extraction and tortuosity evaluation: A comprehensive review. IEEE Access **8**, 197787–197816 (2020). https://doi.org/10.1109/ACCESS.2020.3033027
9. Liskowski, P., Krawiec, K.: Segmenting retinal blood vessels with deep neural networks. IEEE Transactions on Medical Imaging **35**, 2369–2380 (11 2016). https://doi.org/10.1109/TMI.2016.2546227
10. Martinez-Perez, M.E., Hughes, A.D., Thom, S.A., Bharath, A.A., Parker, K.H.: Segmentation of blood vessels from red-free and fluorescein retinal images. Medical Image Analysis **11**(1), 47–61 (2007). https://doi.org/10.1016/j.media.2006.11.004
11. Mendonça, A.M., Campilho, A.: Segmentation of retinal blood vessels by combining the detection of centerlines and morphological reconstruction. IEEE Transactions on Medical Imaging **25**, 1200–1213 (9 2006). https://doi.org/10.1109/TMI.2006.879955
12. Palomera-Pérez, M.A., Martinez-Perez, M.E., Benítez-Pérez, H., Ortega-Arjona, J.L.: Parallel multiscale feature extraction and region growing: Application in retinal blood vessel detection. IEEE Transactions on Information Technology in Biomedicine **14**, 500–506 (3 2010). https://doi.org/10.1109/TITB.2009.2036604
13. Sawalha, S., Awajan, A.: Blank background image lossless compression technique. International Journal of Image Processing (IJIP) **8**, 9–16 (02 2014)
14. Staal, J., Abràmoff, M.D., Niemeijer, M., Viergever, M.A., Ginneken, B.V.: Ridge-based vessel segmentation in color images of the retina. IEEE Transactions on Medical Imaging **23**, 501–509 (4 2004). https://doi.org/10.1109/TMI.2004.825627
15. Yang, C.W., Ma, D., Chao, S., Wang, C., Wen, C.H., Lo, C., Chung, P.C., Chang, C.I.: Computer-aided diagnostic detection system of venous beading in retinal images. Optical Engineering - OPT ENG **39**, 1293–1303 (05 2000). https://doi.org/10.1117/1.602487